Rock Mech. Rock Engng. (2002) 35 (2), 127–137

Rock Mechanics and Rock Engineering

Technical Note
Wedge Stability Analysis Considering Dilatancy of Discontinuities

By

Y.-J. Wang and **J.-H. Yin**

Department of Civil and Structural Engineering, The Hong Kong Polytechnic University, Hong Kong, China

1. Introduction

The stability analysis of a wedge formed by two intersecting discontinuities is often encountered in engineering practice. When establishing spatial force equilibrium equations for this problem, the forces acting on each discontinuity plane involve three unknowns, that is, the magnitude of normal force, the magnitude and direction of shear force (tangential force). For two discontinuities there are 6 unknowns. The magnitude of factor of safety is an additional unknown. However, the number of force equilibrium equations for a wedge is only three. If assuming that the forces on each of two discontinuity planes follow the Mohr-Coulomb failure criterion, then two additional equations are available. Therefore, there are a total of 5 equations with 7 unknowns. Thus, the wedge problem is statically indeterminate and two assumptions must be made to render this problem statically determinate.

Generally, the conventional method for the wedge stability analysis based on the limit force equilibrium assumes the direction of potential sliding of a wedge is parallel to the line of intersection (Wittke, 1967; Hoek et al., 1973; Hoek et al., 1973; Hoek and Bray, 1977; Jaeger, 1971; Goodman, 1995; Low 1997; Kumsar et al., 2000). The assumption made in the conventional method actually implies that the direction of shear force is also parallel to the line of intersection. Using the upper bound method, Chen (1999) and Chen et al. (1999) questioned the assumption and found that the factor of safety for a wedge of cohesive material (zero friction angle) is the same as obtained from the conventional method. However, for a wedge with cohesionless material, the difference in the factor of safety between the upper bound method and the conventional method is obvious.

This paper deals with a method for calculation of the factor of safety by using the limit equilibrium method and considering the dilatancy of discontinuities on which the wedge rests. The direction of shear force on each discontinuity plane is determined by considering the dilative movement along the discontinuous plane. The variation of factor of safety with a dilative coefficient (or the direction of shear force) is also investigated.

2. Wedge Geometry and Forces Acting on the Wedge

In this paper, a wedge formed by two intersecting discontinuity planes is considered (as shown in Fig. 1). For clarity, the wedge itself is taken away as shown in Fig. 1. The flatter discontinuity plane is identified as Plane 1 and the right steeper as Plane 2. The orientations of top surface, slope surface, Planes 1 and 2 are represented by their dip directions and dip angles respectively. The height of the wedge, H, is defined as the difference in elevations at Point A and Point B. A local cartesian coordinate system (h, q, g) is defined as follows: the q-axis is in the direction of the line of intersection of the two discontinuities; the g-axis, which is lied in the vertical plane through the q-axis, is perpendicular to q-axis; the h-axis is perpendicular to the plane through the q-axis and g-axis. The unit vectors along axes $\boldsymbol{h}$, $\boldsymbol{q}$ and $\boldsymbol{g}$ are denoted by the same bold lower-case letters $\boldsymbol{h}$, $\boldsymbol{q}$ and $\boldsymbol{g}$ respectively. Their direction cosines in (x, y, z) coordinate system are denoted by (h_x, h_y, h_z), (q_x, q_y, q_z) and (g_x, g_y, g_z), respectively.

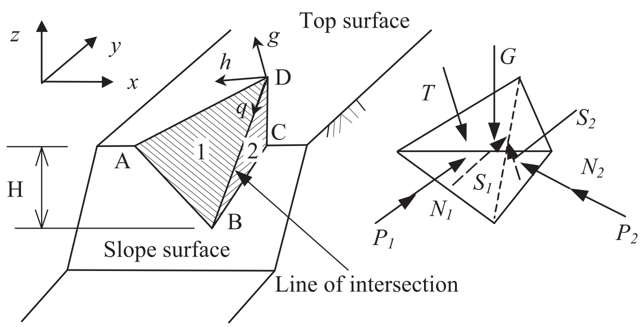

Fig. 1. Isometric view of a wedge and the forces acting on the wedge

The forces acting on the wedge are shown in Fig. 1 and summarised as follows:

- The normal reactions N_1 and N_2 applied on discontinuity Planes 1 and 2 respectively.
- The shear forces S_1 and S_2 acting on the discontinuity Planes 1 and 2 respectively. The water pressures P_1 and P_2 are considered on Planes 1 and 2.
- The weight of the wedge is denoted as G, direction cosines of which are $(0, 0, -1)$.
- A total external force T, which is the resultant of all external forces acting on the surfaces of the wedge regardless of their distribution is considered. The direction of T is specified in advance in the analysis. The unit vector in the direction of T and the direction cosines are denoted by bold lower-case letter $\boldsymbol{t}$ and (t_x, t_y, t_z), respectively.

For a specified geometry of a wedge and distribution of external forces, there are totally 7 unknowns in the analysis of wedge stability using the limit force equilibrium method. These magnitudes of N_1, N_2, S_1 and S_2, directions of S_1 and S_2, and factor of safety F. However, there are only 5 equations, that is, 3 spatial static force equilibrium equations and two equations of the Mohr-Coulomb failure criterion relating the normal force and the shear force.

3. Determination of Direction of Potential Sliding

The shear behaviour of discontinuity is concerned in rock mechanics practice (Brady and Brown, 1985; Wittke, 1990). Experimental results have shown that, in the process of shearing, a discontinuity plane exhibits strong dilatancy due to the roughness of discontinuity surfaces. The results indicate that the upper rock mass moves upward during shearing represented by relative velocity $\boldsymbol{V}$ (see Fig. 2), which inclines at an angle of dilatancy, ψ, from the lower rock mass on the discontinuity surface in average. It is generally advantageous to describe the relative displacement at a discontinuity plane in terms of the normal and shear strain rates or relative velocity (Wittke, 1990). Generally, the angle of dilatancy ψ ranges from zero to the friction angle ϕ ($0 \leq \psi \leq \phi$) on the discontinuity surface or joint. In the case of two-dimensional shearing of discontinuity, the direction of frictional shear force on a block, which is dependent on the relative movement of discontinuity, is parallel to the direction of the relative velocity projected on the discontinuity surface (180° from the projected direction). Similarly, the extension of the two-dimensional observation to a three-dimensional case suggests that the direction of the frictional shear force on the wedge is parallel to, but 180° from the direction of the projection of the relative velocity $\boldsymbol{V}$ on the discontinuity plane. Therefore, the shear force, normal to discontinuity plane and relative velocity should lie on the same plane.

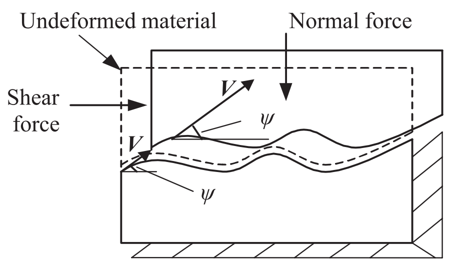

Fig. 2. Relative displacement of the discontinuity plane under shear loading

Figure 3 shows typical movement of a wedge and the wedge velocity $\boldsymbol{V}$, which inclines at angle of dilatancy ψ_1 with respect to the left discontinuity Plane 1 and at ψ_2 to the right discontinuity Plane 2. The components of the velocity vector of the wedge in the (x, y, z) coordinate system are denoted by (v_x, v_y, v_z). Likewise, the unit vector $\boldsymbol{n}_1$ normal to the left discontinuity Plane 1 is denoted by (n_{1x}, n_{1y}, n_{1z}); the unit vector $\boldsymbol{n}_2$ normal to the right discontinuity Plane 2 is denoted by

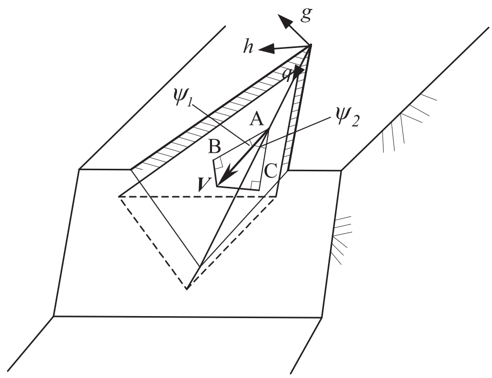

Fig. 3. Velocity diagram of the wedge

(n_{2x}, n_{2y}, n_{2z}). The wedge velocity $\boldsymbol{V}$ inclined at the angle of dilatancy ψ_1 to the left discontinuity surface indicates the angle between the velocity vector $\boldsymbol{V}$ and normal vector $\boldsymbol{n}_1$ to be $\pi/2 - \psi_1$, which yields

$$\Phi(\boldsymbol{V} \cdot \boldsymbol{n}_1) = \cos(\pi/2 - \psi_1) = \sin\psi_1. \tag{1}$$

Similarly, the wedge velocity $\boldsymbol{V}$ inclined at angle of dilatancy $\pi/2 - \psi_2$ with respect to normal vector $\boldsymbol{n}_2$ gives

$$\Phi(\boldsymbol{V} \cdot \boldsymbol{n}_2) = \sin\psi_2, \tag{2}$$

where $\Phi(\boldsymbol{V} \cdot \boldsymbol{n}_i)$ can be determined by

$$\Phi(\boldsymbol{V} \cdot \boldsymbol{n}_i) = \frac{v_x \cdot n_{ix} + v_y \cdot n_{iy} + v_z \cdot n_{iz}}{\sqrt{v_x^2 + v_y^2 + v_x^2} \cdot \sqrt{n_{ix}^2 + n_{iy}^2 + n_{iz}^2}} \quad i = 1, 2. \tag{3}$$

In general, the magnitude of the velocity of a wedge, which is independent of the factor of safety or other variables, is assumed to be unit. Thus

$$|\boldsymbol{V}| = \sqrt{v_x^2 + v_y^2 + v_z^2} = 1. \tag{4}$$

Based on the given value of angle of dilatancy, the three components v_x, v_y and v_z of velocity $\boldsymbol{V}$ can be determined by solving the system of non-linear Eqs. (1), (2) and (4). It should be mentioned here that there are two sets of solutions for the velocity due to Eq. (4). The right one should render potential sliding of the wedge downward and outward rather than that upward and inward.

4. Determination of Direction of Shear Forces and Calculation of Factor of Safety *F*

4.1 Directions of Shear Forces

Two dilative coefficients η_1, η_2, which relate the angles of dilatancy ψ_1 and ψ_2 to the friction angles ϕ_1 and ϕ_2 on the discontinuity surfaces, are defined as

$$\eta_1 = \psi_1/\phi_1, \tag{5}$$

$$\eta_2 = \psi_2/\phi_2. \tag{6}$$

For a set of given dilative coefficients η_1 and η_2, the unit vector of velocity $\boldsymbol{V}(v_x, v_y, v_z)$ can be obtained from Eqs. (1), (2) and (4). The unit vector (S_{1x}, S_{1y}, S_{1z}) of the upward frictional shear force on the left discontinuity surface of the wedge is 180° from the direction of projection of unit vector of velocity $\boldsymbol{V}$ on the left discontinuity surface, and given by vector analysis as

$$\boldsymbol{S}_1 = \frac{\boldsymbol{V} \times \boldsymbol{n}_1 \times \boldsymbol{n}_1}{|\boldsymbol{V} \times \boldsymbol{n}_1 \times \boldsymbol{n}_1|}. \tag{7}$$

Similarly, the unit vector (S_{2x}, S_{2y}, S_{2z}) of upward shear force on the right discontinuity surface is given by

$$\boldsymbol{S}_2 = \frac{\boldsymbol{V} \times \boldsymbol{n}_2 \times \boldsymbol{n}_2}{|\boldsymbol{V} \times \boldsymbol{n}_2 \times \boldsymbol{n}_2|}. \tag{8}$$

In general, the factor of safety, F, is defined as

$$F = \frac{c}{c_e} = \frac{\tan\phi}{\tan\phi_e}, \tag{9}$$

where c and ϕ denote cohesion and friction angle on the discontinuity surfaces (or joints) respectively, c_e and ϕ_e are the mobilised cohesion and friction angle.

Correspondingly, two mobilised dilative coefficients, η_{e1}, η_{e2}, which relate the angles of dilatancy ψ_1 and ψ_2 to the mobilised friction angles ϕ_{e1} and ϕ_{e2}, are defined as

$$\eta_{e1} = \psi_1/\phi_{e1}, \tag{10}$$

$$\eta_{e2} = \psi_2/\phi_{e2}. \tag{11}$$

Theoretically, the mobilised dilative coefficients, η_{e1}, η_{e2}, which increase with the increase in dilative coefficients, η_1, η_2 and come to a value of 1 prior to η_1, η_2. This indicates that $0 \le \eta_{e1}, \eta_{e2} \le 1$. The value 1 of η_{e1}, (or η_{e2}) means that the material follows an associated flow rule.

4.2 Determination of Factor of Safety F

Referring to Fig. 1, three force equilibrium equations can be established along the three axes of local coordinate system (h, q, g) as follows.

Force equilibrium equation in the direction of h-axis:

$$(N_1 + P_1)l_1 + (N_2 + P_2)l_2 + S_1 l_3 + S_2 l_4 + T l_5 = 0, \tag{12}$$

where $l_1 = \boldsymbol{n_1} \cdot \boldsymbol{h} = n_{1x} \cdot h_x + n_{1y} \cdot h_y + n_{1z} \cdot h_z$, $l_2 = \boldsymbol{n_2} \cdot \boldsymbol{h} = n_{2x} \cdot h_x + n_{2y} \cdot h_y + n_{2z} \cdot h_z$, $l_3 = \boldsymbol{S_1} \cdot \boldsymbol{h} = S_{1x} \cdot h_x + S_{1y} \cdot h_y + S_{1z} \cdot h_z$, $l_4 = \boldsymbol{S_2} \cdot \boldsymbol{h} = S_{2x} \cdot h_x + S_{2y} \cdot h_y + S_{2z} \cdot h_z$, $l_5 = \boldsymbol{t} \cdot \boldsymbol{h} = t_x \cdot h_x + t_y \cdot h_y + t_z \cdot h_z$.

Force equilibrium equation in the direction of q-axis:

$$(N_1 + P_1)m_1 + (N_2 + P_2)m_2 + S_1 m_3 + S_2 m_4 + T m_5 = G q_z, \tag{13}$$

where $m_1 = \boldsymbol{n_1} \cdot \boldsymbol{q} = n_{1x} \cdot q_x + n_{1y} \cdot q_y + n_{1z} \cdot q_z$, $m_2 = \boldsymbol{n_2} \cdot \boldsymbol{q} = n_{2x} \cdot q_x + n_{2y} \cdot q_y + n_{2z} \cdot q_z$, $m_3 = \boldsymbol{S_1} \cdot \boldsymbol{q} = S_{1x} \cdot q_x + S_{1y} \cdot q_y + S_{1z} \cdot q_z$, $m_4 = \boldsymbol{S_2} \cdot \boldsymbol{q} = S_{2x} \cdot q_x + S_{2y} \cdot q_y + S_{2z} \cdot q_z$, $m_5 = \boldsymbol{t} \cdot \boldsymbol{q} = t_x \cdot q_x + t_y \cdot q_y + t_z \cdot q_z$.

Force equilibrium equation in the direction of g-axis:

$$(N_1 + P_1)k_1 + (N_2 + P_2)k_2 + S_1k_3 + S_2k_4 + Tk_5 = Gg_z, \tag{14}$$

where $k_1 = \boldsymbol{n_1} \cdot \boldsymbol{g} = n_{1x} \cdot g_x + n_{1y} \cdot g_y + n_{1z} \cdot g_z$, $k_2 = \boldsymbol{n_2} \cdot \boldsymbol{g} = n_{2x} \cdot g_x + n_{2y} \cdot g_y + n_{2z} \cdot g_z, k_3 = \boldsymbol{S_1} \cdot \boldsymbol{g} = S_{1x} \cdot g_x + S_{1y} \cdot g_y + S_{1z} \cdot g_z, k_4 = \boldsymbol{S_2} \cdot \boldsymbol{g} = S_{2x} \cdot g_x + S_{2y} \cdot g_y + S_{2z} \cdot g_z$, $k_5 = \boldsymbol{t} \cdot \boldsymbol{g} = t_x \cdot g_x + t_y \cdot g_y + t_z \cdot g_z$.

Generally, magnitudes of the shear forces S_1, S_2 on the discontinuity planes are related to the normal forces N_1, N_2 on the same discontinuity planes by the Mohr-Coulomb failure criterion, that is,

$$S_1 = c_{e1}A_1 + N_1 \tan\phi_{e1}, \tag{15}$$

$$S_2 = c_{e2}A_2 + N_2 \tan\phi_{e2}. \tag{16}$$

In Eqs. (15) and (16) A_1 and A_2 are the areas of the left and right discontinuity surfaces respectively.

Substituting of Eqs. (15) and (16) into Eqs. (12), (13) and (14) and rearranging yields

$$a_1N_1 + a_2N_2 + (a_3 + l_1N_1 + l_2N_2)F + a_4 = 0, \tag{17}$$

where $a_1 = \tan\phi_1 \cdot l_3$, $a_2 = \tan\phi_2 \cdot l_4$, $a_3 = P_1 \cdot l_1 + P_2 \cdot l_2 + T \cdot l_5$, $a_4 = c_1 \cdot A_1 \cdot l_3 + c_2 \cdot A_2 \cdot l_4$.

$$b_1N_1 + b_2N_2 + (b_3 + m_1N_1 + m_2N_2)F + b_4 = 0, \tag{18}$$

where $b_1 = \tan\phi_1 \cdot m_3$, $b_2 = \tan\phi_2 \cdot m_4$, $b_3 = P_1 \cdot m_1 + P_2 \cdot m_2 + T \cdot m_5 - G \cdot q_z$, $b_4 = c_1 \cdot A_1 \cdot m_3 + c_2 \cdot A_2 \cdot m_4$.

$$d_1N_1 + d_2N_2 + (d_3 + k_1N_1 + k_2N_2)F + d_4 = 0, \tag{19}$$

where $d_1 = \tan\phi_1 \cdot k_3$, $d_2 = \tan\phi_2 \cdot k_4$, $d_3 = P_1 \cdot k_1 + P_2 \cdot k_2 + T \cdot k_5 - G \cdot g_z$, $d_4 = c_1 \cdot A_1 \cdot k_3 + c_2 \cdot A_2 \cdot k_4$.

Note that the normal forces N_1, N_2 and factor of safety F are only involved in Eqs. (17), (18) and (19), which are a system of nonlinear equations with variables N_1, N_2 and F. These three unknowns can be determined by the general method of solving a system of nonlinear equations (Press et al., 1988). Then, the mobilised dilative coefficients, η_{e1}, η_{e2}, are determined by using Eqs. (10) and (11).

5. Hoek and Bray's Example

The variation of the factor of safety with various combinations of dilative coefficients is investigated by using an example presented by Hoek and Bray (1977). The wedge geometry and material strength parameters are listed in Table 1. Values of the factor of safety determined by the present method are summarised in Table 2. The variation of mobilised dilative coefficients, η_{e1}, η_{e2}, with dilative coefficients, η_1, η_2, are also listed in Table 3 and Table 4, respectively.

Table 1. Wedge geometry and material strength parameters

Plane	Dip direction (°)	Dip(°)	Properties
Discontinuity 1	105	45	$c_1 = 23.9$ kN/m^2 (500 lb/ft^2), $\phi_1 = 20°$
Discontinuity 2	235	70	$c_2 = 47.9$ kN/m^2 (1000 lb/ft^2), $\phi_2 = 30°$
Slope surface	185	65	$\gamma = 25.2$ kN/m^3 (160 lb/ft^3), $\gamma_w = 9.81$ kN/m^3 (62.5 lb/ft^3)
Top surface	195	12	height = 30.48 m (100 ft)

After Hoek and Bray (1977) and water pressure not considered.

Table 2. Variation of factor of safety F with dilative coefficients η_1, η_2

F (η_1 \ η_2)	0.0	0.1	0.2	0.3	0.4	0.5	0.555
0.0	1.846	1.863	1.877	1.889	1.898	1.905	1.907
0.1	1.857	1.873	1.887	1.898	1.906	1.913	1.915
0.2	1.866	1.882	1.895	1.906	1.914	1.919	1.921
0.3	1.874	1.889	1.902	1.912	1.919	1.924	1.926
0.4	1.881	1.896	1.907	1.917	1.923	1.927	1.929
0.5	1.886	1.900	1.911	1.920	1.926	1.929	1.930
0.534	1.888	1.902	1.913	1.921	1.927	1.930	1.930

Table 3. Variation of mobilised dilative coefficient η_{e1} with dilative coefficients η_1, η_2

η_{e1} (η_1 \ η_2)	0.0	0.1	0.2	0.3	0.4	0.5	0.555
0.0	0	0	0	0	0	0	0
0.1	0.180	0.182	0.183	0.184	0.185	0.186	0.186
0.2	0.363	0.365	0.368	0.370	0.372	0.372	0.373
0.3	0.546	0.550	0.554	0.557	0.559	0.560	0.561
0.4	0.731	0.736	0.740	0.744	0.746	0.748	0.749
0.5	0.916	0.922	0.927	0.832	0.934	0.936	0.936
0.534	0.979	0.986	0.991	0.995	0.999	1.000	1.000

Table 4. Variation of mobilised dilative coefficient η_{e2} with dilative coefficients η_1, η_2

η_{e2} (η_1 \ η_2)	0.0	0.1	0.2	0.3	0.4	0.5	0.555
0.0	0	0.174	0.351	0.530	0.709	0.890	0.988
0.1	0	0.175	0.353	0.532	0.712	0.893	0.992
0.2	0	0.176	0.354	0.534	0.715	0.896	0.995
0.3	0	0.177	0.355	0.536	0.717	0.898	0.998
0.4	0	0.177	0.356	0.537	0.718	0.899	0.999
0.5	0	0.177	0.357	0.538	0.719	0.900	1.000
0.534	0	0.178	0.357	0.538	0.719	0.901	1.000

From Table 2, the factor of safety for the case of $\eta_1 = \eta_2 = 0$ ($\eta_{e1} = \eta_{e2} = 0$) is 1.846, which is identical to that obtained by Hoek and Bray (1977). However, when the angle of dilatancy is not equal to zero, but varies from zero to the mobilised friction angle ($0 < \eta_{e1}, \eta_{e2} < 1$), the value of the factor of safety varies accordingly. The factor of safety, F, is equal to 1.846 (the minimum) at $\eta_{1e1} = \eta_{e1} = 0.0$. The F then slowly increases with the increase in the mobilised dilative coefficients and arrives at the maximum value of 1.930 at $\eta_{e1} = 1.0$, $\eta_{e2} = 1.0$ ($\eta_1 = 0.534$, $\eta_2 = 0.555$) (see Table 2). Since the change in mobilised dilative coefficients means the change in the direction of shear forces on the discontinuity surfaces. This implies that the change in direction of shear forces has considerable influence on the factor of safety. It is noted that $\eta_{e1} = 1.0$ and $\eta_{e2} = 1.0$ mean that the joint materials follow an associated flow rule. The factor of safety reaches the maximum value of 1.930 at $\eta_{e1} = 1.0$, $\eta_{e2} = 1.0$ ($\psi_1 = \phi_{e1}$ and $\psi_2 = \phi_{e2}$) when using an associated flow rule. The directions of shear forces on discontinuity surfaces corresponding to the maximum value of the factor of safety can be determined. In this example, the angles between the directions of shear forces on left and right discontinuity surfaces are 19.4° and 14.7° for $\eta_{e1} = 1.0$, $\eta_{e2} = 1.0$ ($\eta_1 = 0.534$, $\eta_2 = 0.555$), respectively.

6. A Symmetrical Wedge

To further investigate the wedge problem, a wedge symmetrical in geometry is analysed. The cohesion and friction angles associated with two slip surfaces are the same. The wedge geometry and material strength parameters are listed in Table 5. Values of the factor of safety determined by the present method are summarised in Table 6.

From Table 6, the factor of safety obtained using the conventional method and in the case of $\eta_e = \eta = 0$ using the present method is the same and equal to 1.229 with zero dilation. However, the maximum value of factor of safety is 1.4297 at $\eta_e = 1.0$ ($\eta = 0.733$) where the angle between the shear force on the slip surface and the line of intersection is 30.7°. The difference in the values of the factor of safety for the two cases is about 0.2. Accordingly, the factor of safety, F, increases with the mobilised dilative coefficient, reaches the maximum at $\eta_e = 1.0$ with fully mobilised dilation.

Table 5. Geometry and strength parameters for a symmetrical wedge

	Dip Direction (°)	Dip (°)	Cohesion c (kPa)	Friction angle ϕ (°)	
Left discontinuity surface	120	65	10	30	$\gamma = 26.64$ kN/m^3 H = 10.2 m
Right discontinuity surface	240	65	10	30	
Top surface	180	0			
Slope surface	180	90			

Table 6. Variation of factor of safety with η and η_e

Dilative coefficient η	Mobilised dilative coefficient η_e	Factor of safety F
0.0	0.0	1.229
0.1	0.123	1.274
0.2	0.253	1.315
0.3	0.389	1.350
0.4	0.529	1.380
0.5	0.671	1.404
0.6	0.814	1.421
0.7	0.955	1.429
0.733	1.000	1.4297

Water pressure not considered.

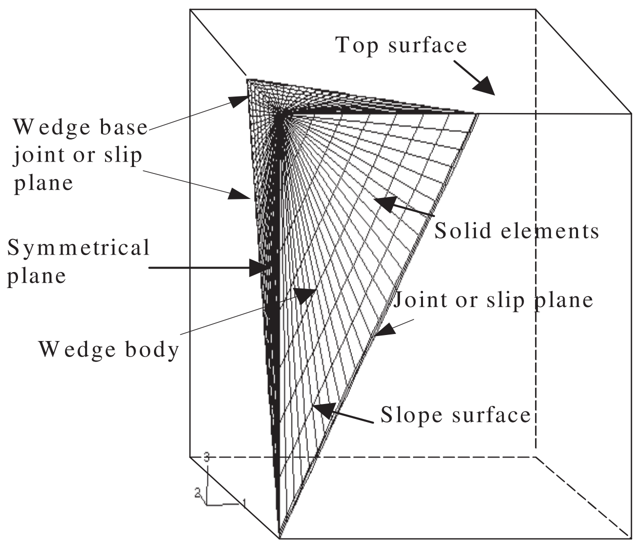

Fig. 4. A three-dimensional finite-element model for the symmetrical wedge problem

In addition, a three-dimensional finite element (FE) model has recently been developed and used by the authors for analysis of the symmetrical wedge using a commercial software (ABAQUS, 1998). Due to the symmetry in geometry of wedge, only the right-hand half of the wedge is analysed. As shown in Fig. 4, the wedge is divided into three parts:

(i) the wedge body itself above the slip planes – the main body of the wedge is represented by solid elements and considered to be fully elastic, since we are interested in stability only, not deformation.
(ii) the slip plane – the slip plane is simulated by a very thin layer of solid elements of a material that follows the Mohr-Coulomb criterion.

(iii) the base beneath the slip planes – the base is simulated as a rigid body and can be simplified as fixed supports since we are interested in stability only.

The nodes on the symmetrical plane are not allowed to move in the x direction (numbered as 1). A value of the factor of safety of the wedge problem is determined when the normal and tangential components of reaction forces of the wedge base node forces along the two slip planes fully satisfy the Mohr-Coulomb failure criterion for a given combination of cohesion and friction angle of the slip plane material.

For the symmetrical wedge problem with $c = 10$ kPa and $\phi = 30°$, the factor of safety determined by the FE analysis is 1.430 very close to 1.4297 at $\eta_e = 1.0$ using the present method. The angle between the shear force and line of intersection is about 29.9° using the FE method, which is also close to 30.7° determined by the proposed method. The results obtained by the three-dimensional finite-element analysis support the proposed simple method in two aspects: (a) the direction of the shear force inclines at a certain angle with respect to the line of intersection and (b) the factor of safety is greater than that obtained by the conventional method for wedge analysis if dilation is not zero.

7. Conclusions

Based on the results and discussion presented above, the following conclusions may be drawn:

- The factor of safety, F, varies for different combination of η_{e1} and η_{e2} (or mobilised dilation angles). The F has the minimum value for $\eta_{e1} = 0$ and $\eta_{e2} = 0$ and is the same as that obtained using the conventional method. The F reaches the maximum value for $\eta_{e1} = 1$ and $\eta_{e2} = 1$. The difference in the values of the factor of safety for (a) $\eta_{e1} = 1$ and $\eta_{e2} = 1$ and (b) $\eta_{e1} = 0$ and $\eta_{e2} = 0$ is apparent.
- The factor of safety is dependent on the directions of shear forces on the discontinuities and the dilation angle of the discontinuities.
- The conventional method assuming the direction of shear force is in the direction the line of intersection, to some extent, underestimates the factor of safety if the dilation exists.
- The proposed method is a simple method for wedge analysis when considering the dilatancy of the discontinuities.

It shall be pointed out that the dilatancy at the joints or the discontinuity is dependent on the effective surface morphology and may be anisotropic (Aydan et al., 1996). The treatment of the dilatancy in a way similar to soil mechanics in this paper is a phenomenological and simple approach without consideration of the surface morphology. However, the work done by Aydan et al. (1996) is very valuable. It is thought that the proposed method may be extended to consider the anisotropic dilatancy as studied by Aydan et al. (1996) in a future study.

Acknowledgements

The research and preparation of this paper have received financial supports from a RGC (Research Grants Council) grant (PolyU 5064/00E) of the University Grants Committee of the Hong Kong Special Administrative Region Government of China and the Hong Kong Polytechnic University. These financial supports are gratefully acknowledged.

References

ABAQUS (1998): Theory and users manual, Version 5.8. Hibbit, Karlsson and Sorensen Inc., Pawtucket, USA.

Aydan, Ö., Shimizu, Y., Kawamoto, T. (1996): The anisotropy of surface morphology and shear strength characteritics of rock discontinuities and its evaluation. Proc., 2nd North American Rock Mechanics Symposium, NARSM'96, 1391–1398.

Brady, B. H. G., Brown, E. T. (1985): Rock mechanics for underground mining. George Allen & Unwin, London, UK.

Chen, Z. Y. (1999): The limit analysis for slopes: theory, methods and applications. In: Yagi, N., Yamagami, T., Jiang, J.-C. (eds.) Slope stability engineering. Balkema, Rotterdam, 15–29.

Chen, Z. Y., Wang, Y. J., Wang, X. G., Wang, J. (1999): An upper bound wedge failure analysis method. In: Yagi, N., Yamagami, T., Jiang, J.-C. (eds.), Slope stability engineering. Balkema, Rotterdam, 325–328.

Goodman, R. E. (1995): Thirty-fifth Rankine lecture. Block theory and its application. Geotechnique 45(3), 383–423.

Hoek, E. (1973): Methods for the rapid assessment of the stability of three-dimensional rock slopes. Quarterly J. Engng. Geol. 6, 243–255.

Hoek, E., Bray, J. W. (1977): Rock slope engineering. Inst. Min. Metallurgy, London.

Hoek, E., Bray, J. W., Boyd, J. M. (1973): The stability of a rock slope containing a wedge resting on two intersecting discontinuities. Quarterly J. Engng. Geol. 6(1), 1–55.

Jaeger, J. C. (1971): Friction of rocks and the stability of rock slope. Geotechnique. 21(2), 97–134.

Kumsar, H., Aydan, Ö., Ulusay, R. (2000): Dynamic and Static stability of rock slopes against wedge failures. Rock Mech. Rock Engng. 33(1), 31–51.

Low, B. K. (1997): Reliability analysis of rock wedges. ASCE J. Geotech. Geoenvironm. Engng. 123(6), 498–505.

Press, W. H., Flannery, B. P., Teukolsky, S. A., Vetterling, W. T. (1988): Numerical recipes: the art of scientific computing. Cambridge University Press, Cambridge.

Wittke, W. (1967): Influence of the shear strength of the joints on the design of prestressed anchors to stabilize a rock slop. Geotechnical Conference, Oslo, Paper No. 4.11, 311–318.

Wittke, W. (1990): Rock mechanics: theory and applications with case histories. Springer, Wien Heidelberg New York Tokyo.

Authors' address: Assoc. Prof. Jian-Hua Ying, Department of Civil and Structural Engineering, The Hong Kong Polytechnic University, Hung Hom, Kowloon, Hong Kong, China. E-mail: cejhyin@polyu.edu.hk.